Pharm Res (2014) 31:489–499
DOI 10.1007/s11095-013-1177-2

RESEARCH PAPER

Prediction of H3 Receptor Occupancy Diurnal Fluctuations Using Population Modeling and Simulation with Focus on Guiding Dose Selection in a Phase IIa Study

Emma Boström • Yi-Fang Cheng • Niclas Brynne • Märta Segerdahl

Received: 19 September 2012 / Accepted: 9 August 2013 / Published online: 28 September 2013

ABSTRACT

Purpose 4-[(1S,2S)-2-(4-cyclobutylpiperazine-1-carbonyl) cyclopropyl]benzamide ("AZ1") is a histamine 3 (H3) autoreceptor *in vivo* antagonist. Sleep disturbance is a well-known class-effect for H3 antagonists and associated with high H3 receptor occupancy (RO) at night. The objective of the present work was to investigate if it was possible to obtain large diurnal fluctuations in RO for AZ1 and to suggest suitable doses for a Phase IIa study.

Methods Four Phase I studies were pooled and used to build a population pharmacokinetic model in NONMEM. Based on simulations of the PK model and the reported Ki-value for H3 RO from a human PET-study, RO *vs*. time profiles were simulated.

Results The model well described the AZ1 pharmacokinetics. Simulations predicting plasma concentration and RO *vs*. time profiles for several doses were explored and doses with a wide range of fluctuation in RO over the dosing interval could be identified.

Conclusions By using population modeling and simulations of PK data and the Ki-value from a human PET study, predictions of RO *vs*. time for unstudied doses of AZ1 was made. Using this methodology it was possible to suggest doses with expected large diurnal fluctuations in RO.

KEY WORDS histamine · NONMEM · population modeling · receptor occupancy · simulation

ABBREVIATIONS

ACh	Acetylcholine
AD	Alzheimer's disease
AZ1	4-[(1S,2S)-2-(4-cyclobutylpiperazine-1-carbonyl)cyclopropyl]benzamide
CL	Clearance
CL/F	Oral clearance
CNS	Central nervous system
C_{trough}	Minimal plasma concentration during a dosing interval
CV	Coefficient of variation
DA	Dopamine
JSMAD	Single and multiple ascending dose in Japanese subjects
KA	Absorption rate constant
Ki	Plasma concentration yielding 50% RO
LLOQ	Lower limit of quantification
MAD	Multiple ascending dose
OFV	Objective function value
PD	Parkinson's disease
PET	Positron emission tomography
PI	Prediction interval
PK	Pharmakokinetics
PKPD	Pharmacokinetic / Pharmacodynamic
Q/F	Oral intercompartmental clearance
RO	Receptor occupancy
RO_{max}	Maximal receptor occupancy during a dosing interval
RO_{trough}	Minimal receptor occupancy during a dosing interval
SAD	Single ascending dose
t1/2	Plasma half-life
V	Volume of distribution
V2/F	Oral central volume of distribution
V3/F	Oral peripheral volume of distribution
VPC	Visual predictive check

Electronic supplementary material The online version of this article (doi:10.1007/s11095-013-1177-2) contains supplementary material, which is available to authorized users.

E. Boström (✉) • Y.-F. Cheng • N. Brynne • M. Segerdahl
AstraZeneca R&D, 15185 Södertälje, Sweden
e-mail: emma.bostrom@astrazeneca.com

INTRODUCTION

Histamine causes a range of physiological responses mediated by histamine H1, H2, H3 and H4 receptors. H1 and H2

receptors are very widely distributed throughout the body, while H3 auto receptors are predominantly expressed in the brain (1) and the H4 receptor is expressed peripherally in leukocytes (2). Inactivation of the H3 receptor results in increased release of histamine, which is one of the main regulators of sleep by inducing wakefulness via a direct agonism on H1 receptors. Increased histamine levels also enhance attention/vigilance and working memory, likely via activation of H2 receptors. Inactivation of H3 receptors increases release of other neurotransmitters important in cognitive processes such as acetylcholine (ACh), noradrenaline, serotonin and dopamine (DA) (3,4). This multiple transmitter release mechanism has gained the interest of several pharmaceutical companies that now have H3 antagonists under clinical development for the treatment of cognitive impairment associated with a number of diseases, such as Alzheimer's disease (AD), obstructive sleep apnea and Parkinson's disease (PD).

The histamine system serves as the key driver in the maintenance of the waking state, where phasic direct activation of the H1 receptor in the posterior hypothalamus is probably the most important physiological mechanism in the maintenance of wakefulness under normal conditions as well as intermittent challenges (5). Therefore, wakefulness and sleep disturbance/ insomnia, are inherent tolerability issues that need to be closely monitored in the development of an H3 antagonist. It is necessary to be able to balance the intended H1 related daytime wakefulness and precognitive effects induced by increased levels of e.g. ACh and DA with histamine related activation of wakefulness leading to sleep disturbance and insomnia. Insomnia will in turn lead to a secondary fatigue related cognitive impairment. Thus it is likely a key success factor for any H3 antagonist project to identify a dose which enables sufficiently high receptor occupancy (RO) during daytime to ensure procognitive ACh and DA release, while keeping sufficiently low exposure/ receptor occupancy at nighttime. It has not been established at what level of H3 RO gives rise to sleep disturbance, but published information suggest that a night time RO >70% is associated with insomnia (1).

A large number of drugs aiming at the H3 target have recently entered preclinical and clinical trials and are being tested in sleep-wake and cognitive disorders, notably in narcolepsy: ABT-288, BF2.649 (pitolisant), GSK189254, GSK239512, JNJ-17216498, MK-0249, MK-3134, and PF-03654746 (6–9). Because the purpose of such a therapy is to improve daytime waking, vigilance, and cognition without disturbing patients' nocturnal sleep, the choice of compounds with reasonable elimination half-life and therapeutic dose window would be particularly important and requires individualization to prevent possible peripheral and CNS side effects such as overexcitation (e.g. insomnia).

AZ1 (Fig. 1) is a new potent selective and competitive H3 antagonist of the human histamine H3 receptor for potential treatment of cognitive dysfunctions in several CNS disorders

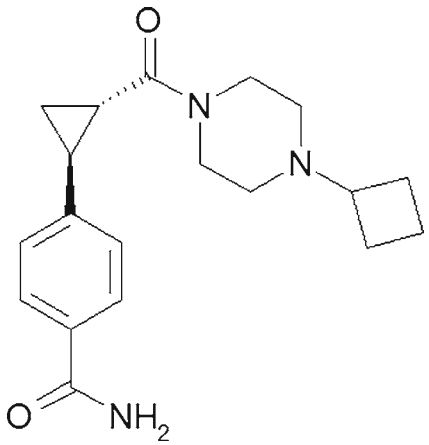

Fig. 1 The chemical structure of AZ1.

such as AD and PD. Pre-clinical studies have shown that AZ1 binds with high affinity to the H3 receptor in both heterogonous and native systems with an *in vitro* K_i of 0.57 nM in human frontal cortex with no affinity for other human histamine receptors (H1, H2 and H4) [AstraZeneca data on file].

AZ1 has been given to healthy volunteers as single doses up to 80 mg and as multiple doses up to 18 mg daily (Lindholm *et al.*, in preparation). The plasma half-life of AZ1 is approximately 5 to 7 h (Lindholm *et al.*, in preparation), i.e. considerable shorter than that of other published H3 antagonist, which have been reported to have t1/2 in the range of 11–14 h (10,11). Generally, AZ1 was well tolerated throughout the dose ranges with nausea, headache as the most common adverse events. Interestingly, AZ1 also showed a clear effect on sleep both after single and multiple doses (Lindholm *et al.*, in preparation).

Using population modeling, the AZ1 plasma concentrations from different studies can be brought together and be described by a model. Based on the pharmacokinetic (PK) model and the Ki-value obtained in a human PET study (13), simulations of the predicted RO *vs*. time profiles for different doses of AZ1 can be made. Given the t1/2 of AZ1, we hypothesize that with AZ1 we may achieve the diurnal fluctuations in RO that allows for high RO during day (for putative cognitive improvement) and low RO during night (for avoidance of sleep disturbances).

In the present study we hypothesized that we would, by integrative use of dose, t1/2, and Ki-value, be able to give guidance in dose selection for AZ1 that would yield a high occupancy during daytime and a range of RO during night. By choosing doses yielding a range of night-time RO, the optimal RO *vs*. time profile for early efficacy studies may be determined.

MATERIALS AND METHODS

Study Data

The population PK data set was based on four Phase I studies in healthy volunteers; a single ascending dose study (SAD), a

multiple ascending dose study (MAD), a positron emission tomography study (PET) and a single and multiple dose study in Japanese subjects (JSMAD) (Table I). The data set included plasma concentrations from all healthy volunteers who received AZ1 — subjects in placebo groups were not included in the analysis.

Demography

In the SAD study, there were 60 healthy volunteers (all males), of which 34 Caucasian subjects, 24 black or African American, one Asian and one American Indian; with mean (range) of age 28 (18–50) years and body weight of 81 (59–98) kg.

In the MAD study, there were 54 healthy volunteers including 36 young (males) and 18 elderly (13 males, 5 females), of which 21 young and 18 elderly Caucasian subjects, 11 black, two Asian and two American Indian/Alaskan native; with mean age of 26 to 35 (range: 19–50) years and mean body weight of 76 to 83 (range: 54–101) kg for the young subjects, and mean age of 70 to 71 (range: 66–76) years and mean body weight of 66 to 79 (range: 51–86) kg for the elderly subjects.

In the JSMAD study, there were 36 Japanese healthy volunteers including 24 young (males) and 12 elderly (6 males, 6 females); with mean (range) of age 28 (20–44) years and body weight of 65 (53–80) kg for the young subjects, and mean (range) of age 69 (65–77) years and body weight of 60 (48–72) kg for the elderly subjects.

In the PET study, there were 7 Caucasian healthy male volunteers with mean (range) of age 25 (20–36) years and body weight of 79 (69–87) kg.

Bioanalytical Assays

Samples for determination of AZ1 concentration in plasma were analyzed by PRA International on behalf of AstraZeneca. AZ1 concentrations in human plasma were determined using liquid-liquid extraction followed by LC-MS/MS. Lower limits of quantitation (LLOQ) was 0.100 nM (low calibration range: 0.100 to 50.0 nM) and 5.00 nM (high calibration range: 5.00–2500 nM), respectively. The overall CV for the QC samples at 3 concentrations for the low calibration range was between 3.5% and 4.9% (SAD), 3.6% and 4.1% (MAD), 3.6% and 7.5% (JSMAD), and 2.7% and 9.8% (PET); for the high calibration range, it was between 2.8% and 3.7% (SAD), 2.0% and 7.3% (MAD), 3.1% and 4.8% (JSMAD), and 1.9% and 2.9% (PET).

PK Data Analysis

The software package NONMEM™, version 7.2.0 (Icon Development Solutions, Ellicott City, MD, USA, 2009) was used for the modeling and R (version 2.13.2, The R Foundation for Statistical Computing) was used for graphical analysis, model diagnostics and statistical summaries. Xpose (version 4.3.2) and Pearl-Speaks-Nonmem (PsN) (version 3.4.2, Dept. of Pharmaceutical Biosciences, Uppsala University, Uppsala, Sweden) were used for model diagnostics and some automated procedures including stepwise covariate model building (scm) and generation of bootstrap results. Berkeley Madonna, version 8.3.11, was used for simulations and graphics based on the final population PK model. The plasma concentration data was log-transformed prior to

Table I Study Characteristics and Blood Sampling Schedule for the Data Constituting the Dataset Used for the Pooled PK Analysis

Study	Doses [mg]	Sampling schedule (h after dose)
SAD[a,b]	0.1, 0.3, 1, 2.5, 5, 10, 20, 30, 50, 80	Pre-dose, 0.3, 0.6, 1, 1.5, 2, 3, 4, 6, 8, 12, 16, 24, 36, 48
MAD[b,c]		
Young panel	1, 3, 6, 10, 14, 18	Day 1 and 12: Pre-dose, 0.3, 0.6, 1, 1.5, 2, 3, 4, 6, 8, 12, 24, 36, 48
		Day 5, 7, 10, 11: Predose
Elderly panel	1, 6, 10	Day 1 and 12: Pre-dose, 0.3, 0.6, 1, 1.5, 2, 3, 4, 6, 8, 12, 24, 36, 48
		Day 5, 7, 10, 11: Predose
JSMAD[b,d]		
Young panel	1, 3, 6, 10	Day 1 and 12: Pre-dose, 0.3, 0.6, 1, 1.5, 2, 3, 4, 6, 8, 12, 24, 36, 48
		Day 5, 7, 10, 11: Predose
Elderly panel	6, 10	Day 1 and 12: Pre-dose, 0.3, 0.6, 1, 1.5, 2, 3, 4, 6, 8, 12, 24, 36, 48
		Day 5, 7, 10, 11: Predose
PET[b,e]	0.05, 0.1, 0.3, 1, 2, 2.5, 10, 30	Pre-dose, 0.3, 0.6, 1, 1.5, 2, 3, 4, 6, 8, 12, 24[f], 36[f], 48[f]

[a] Single ascending dose
[b] Healthy volunteers
[c] Multiple ascending dose
[d] Japanese Single and Multiple ascending dose
[e] Positron emission tomography
[f] Optional sampling

analysis. The First Order Conditional Estimation method (FOCE) was used for estimation of the log-transformed data.

The population PK model building started with exploratory analysis of observed data to suggest a tentative model. Thereafter different structural models and error models were explored, as well as exploration of the statistical model (inclusion of inter-individual and inter-occasion variability). The influence of covariates was explored, and finally the model was refined to obtain the final population PK model.

The inter-individual variability was modeled as:

$$P_i = \widetilde{P}\exp(\eta_{Pi})$$

where P_i represents the value of the pharmacokinetic parameter P for the i^{th} subject, while $\widetilde{P}$ is the population mean of that parameter P in the structural model. The random deviation from that mean is given by η_{Pi}. The ηs were assumed to be normally distributed with a mean of 0 and variance ω_P^2 .

One additional parameter (theta or eta) was added at the time using forward selection and these nested models (the model with and without the additional parameter) were assessed by the criteria described in the "Model Assessment" section. Inter-individual and inter-occasion variability as well as different residual error models were explored. The stepwise covariate model building tool in PsN was used to evaluate covariates, with a forward inclusion of $p < 0.01$, and backwards elimination of $p < 0.001$. Age was evaluated as a categorical covariate (OLD), where OLD was set to 1 if the subject was from the elderly panels (65–80 years) and OLD was 0 if the subject was from the young panels (20–50 years). Categorical covariates sex, race (BLA for Black subjects and JAP for Japanese subjects) and OLD were included using power or a proportional change models to the parameters, while the continuous covariate weight (WT) was modeled using a linear function relating the individual weight to the population mean. Covariates were selected based on scientific plausibility and tested for significance.

Model Assessment

Model comparisons were based on NONMEM objective function values (OFV), goodness-of-fit plots, and precision in parameter estimates. A difference in OFV between two nested models is approximately χ^2-distributed, and a ΔOFV greater than 10.83 (one degree of freedom, i.e. one parameter difference) corresponding to $p < 0.001$ was used to discriminate between models.

Basic goodness of fit plots including population and individual predictions *vs.* observed concentrations, as well as individual predictions *vs*. individual weighted residuals, and the distribution of residuals over time were evaluated. The population predictions were based on the typical population parameters in the final model, and the individual predictions on the empirical Bayes estimates of individual pharmacokinetic parameters. The uncertainty of the model parameter is reported as the relative standard error as obtained from NONMEM. The final model was selected on statistical criteria and diagnostic plots.

To evaluate the stability of the final model parameters and the confidence intervals of the parameters, bootstrap analyses were performed using PsN. Five hundred replicate bootstrap datasets were obtained by resampling with replacement from the original dataset and fitted to the same model to obtain parameters estimates for each replicate. The median and 2.5th and 97.5th percentile confidence intervals for the population parameters are presented.

PsN was used to produce visual predictive checks in order to assess the predictability (in terms of general structure as well as variability components) of the final model. For each VPC, 1000 simulations of the model were executed. As there were few individuals in each dose panel, the prediction corrected VPCs were used (12).

Model Application

The final PK model was implemented in the simulation software Berkeley Madonna. To calculate the predicted H_3 receptor occupancy (RO), the Ki-value corresponding to the plasma concentration yielding 50% RO from the human PET study was used (13). In that study, the Ki-value was determined using Lassen plot and non-linear regression and was reported to be 1.14 nM, with a 95% CI of 0.93–1.35 nM. No inter-individual variability in the Ki-value was reported. The predicted RO was calculated using the formula:

$$RO_{i,pred}(\%) = \frac{Conc_{i,pred}}{\widetilde{Ki} + Conc_{i,pred}} \cdot 100 \quad (1)$$

Where $RO_{i,pred}(\%)$ is the individual predicted receptor occupancy in percent and $Conc_{i,pred}$ is the individual predicted concentration based on the final model. To illustrate impact of uncertainty in the Ki-value, simulations of the reported Ki-value as well as the lower and upper bound of the 95% CI (0.93 nM and 1.35 nM, respectively) were performed. To calculate 90% prediction intervals for selected doses of AZ1, 1000 simulations of RO *vs*. time for each Ki (1.14, 0.93 and 1.35 nM), and each dose for a typical individual were made in Berkeley Madonna. The simulated data was transferred to R for calculations of prediction intervals at pseudo steady-state and for further plotting of graphs.

In addition, to visualize the impact of the plasma t1/2 on the RO *vs*. time profiles, additional simulations in Berkeley Madonna were carried out: The clearance and volume of distribution of AZ1 from the final PK model was used for as the base case. The clearance and volume of distribution was

thereafter doubled or halved, to visualize how the altered t1/2 impacted the RO *vs*. time profiles. The Ki-value is unchanged in all simulations, and the doses studied were 0.5, 2 and 6 mg AZ1. For clarity, these simulations were carried out for a typical individual, i.e. without inter-individual variability.

Sleep Assessment

Quality of sleep was determined every morning during the residential period of the studies. The scale used was a 5-item non-linear semi-quantitative scale, where the healthy volunteers' rated the preceding night's sleep. For calculation purposes, the scoring system of the original quality of sleep scale, including the scale steps 0, 1, 3, 4 and 5, were somewhat modified, to range from 1 to 5, still including the original descriptors. The scale then included the following definitions: "1" = "very poor night with little or no sleep", "2" = "difficult night with several awakenings or a long period without sleep", "3" = fair night with only a few brief (<30 min) awakenings", "4" = "good night with only one brief (<10 min) awakening" and "5" = outstanding night with no awakenings".

To evaluate the relationship between RO at night and the self-assessment of sleep for subjects in the SAD, MAD, PET and JSMAD studies, the predicted individual plasma concentration at 16 h after dose was obtained from the model. The dose was given in the morning, and 16 h later corresponded to 12 pm–1 am, i.e. nighttime. Using Eq. 1, the predicted concentration was used to calculate the individual RO 16 h after dose. The data was divided into four bins, based on quantiles of the predicted RO. The subjective sleep quality measures was

Table II Parameter Estimates of the Final Model. The Parameterization of the Model Parameters are presented as Footnotes

Model parameter	Estimate	RSE (%)[a]	Bootstrap median estimate	Bootstrap CI	
				2.50%	97.50%
ALAG1 (lag time) (h)	0.121	0.02	0.121	0.115	0.157
KA (h^{-1})[b]	2.60	6.2	2.61	2.30	2.97
JAP on KA	2.80	11	2.86	2.20	3.69
CL/F (L/h)[c]	23.16	1.6	23.21	22.45	23.92
WT on CL	0.011	11.5	0.011	0.008	0.013
V2/F (L)[d]	135.4	1.2	135.5	131.9	138.9
WT on V2	0.015	6.5	0.015	0.013	0.016
Q/F (L/h)[e]	0.859	6.9	0.857	0.651	1.055
JAP on Q	0.709	20.8	0.72	0.31	1.26
BLA on Q	1.04	15.8	1.04	0.52	1.63
V3/F (L)[f]	12.24	5.5	12.23	10.67	14.28
JAP on V3	0.518	25.3	0.529	0.229	0.809
BLA on V3	6.32	15.3	6.24	3.12	8.70
Proportional error	0.121	1.57	0.120	0.112	0.128
ω CL/F (%)	19.5	12.0	19.3	16.9	22.0
Covariance CL/V2	13.4	15.3	13.2	11.0	15.7
ω V2/F (%)	13.3	13.0	13.1	11.5	14.9
ω V3/F (%)	38.7	16.6	37.7	28.8	44.9
ω KA (%)[g]	76.3	11.2	75.4	64.2	88.9
ω ALAG1 (%)[g]	61.2	13.9	60.7	42.5	69.5
ω CL/F (%) [g]	4.72	12.8	4.7	3.6	6.0

[a] Relative standard error

[b] $TVKA = TH(KA) \cdot TH(KA:JAP)^{JAP}$ where JAP is 1 of the subject is of Japanese race, and 0 if not of Japanese race

[c] $TVCL = TH(CL) \cdot (1 + TH(CL:WT) \cdot (WT - 72.20))$

[d] $TV2 = TH(V2) \cdot (1 + TH(V2:WT) \cdot (WT - 72.20))$

[e] $TVQ = TH(Q) \cdot QBLA \cdot QJAP$ where $QBLA = 1$ if the subject is not of black race and $QBLA = 1 + TH(Q:BLA)$ if the subject is of black race, and $QJAP = 1$ if the subject is not of Japanese race and $QJAP = 1 + TH(Q:JAP)$ if the subject is of Japanese race

[f] $TV3 = TH(V3) \cdot V3BLA \cdot V3JAP$ where $V3BLA = 1$ if the subject is not of black race and $V3BLA = 1 + TH(V3:BLA)$ if the subject is of black race, and $V3JAP = 1$ if the subject is not of Japanese race and $V3JAP = 1 + TH(V3:JAP)$ if the subject is of Japanese race

[g] Inter-occasion variability, where one occasion was the rich sampling on day 1–2, one occasion the rich sampling on the last day of the multiple dose studies and one occasion the days with through sampling.

categorized into level 1–2 (poor sleep) and 3–4–5 (good sleep), in accordance with the original description of the interpretation of the sleep assessment scale. The proportion of level 1–2 responses was plotted against the median RO of each bin, using R.

RESULTS

Population PK Model

A population PK model was developed based on the plasma data from the healthy volunteer data. The total number of subjects included in the analysis was 157 and the total number of plasma concentration observations was 3583. The final model consisted of a 2-compartment disposition model with a relative bioavailability parameter and a 1st order absorption rate constant. A lag time was incorporated in the absorption part of the model. Basic goodness of fit plots of the final model are presented as Supplementary Materials and the population PK parameter estimates of the final model are presented in Table II.

Inter-individual variability was incorporated onto CL/F, V2/F and V3/F. Inter-occasion variability was incorporated onto KA, the lag-time (ALAG1) and CL/F, where one occasion was the rich sampling on day 1–2, one occasion the rich sampling on the last day of the multiple dose studies and one occasion the days with through sampling. Thereby CL/F was allowed variability both between individuals and between different occasions in the same individual. ETA shrinkage of the inter-individual variability in CL/F was low, approximately 2.6%. The residual error was described with a proportional error model.

Covariate relationships that met the statistical significance criteria were identified. KA was found to vary with Japanese race (~2.8-fold increase), included as a power relationship. CL/F and V2/F were both dependent on WT where WT was modeled using a linear function relating the individual weight to the population mean. Weight was not found to be a significant covariate for Q/F and V3/F, but rather on race; both Japanese and Black subjects had different Q/F compared to Caucasians — (Japanese ~71% increase and Black ~104% increase) and V3/F (Japanese ~52% increase and Blacks ~630% increase), included as proportional change to the parameters. The inclusion of race on Q/F and V3/F resulted in a large drop in OFV, as presented in Table III. The parameterization of the parameters is presented in Table II.

The stability of the final model parameter estimates was evaluated by running 500 bootstrap replicates. The bootstrap parameter estimates and the 2.5% and 97.5% confidence intervals are presented in Table II, and show that the parameter estimates were stable.

Visual predictive checks were performed for the final model using PsN. Due to the small number of individuals in each dose panel, the VPCs were prediction corrected (12). Figure 2 shows the prediction corrected plasma concentration *vs*. time on log scale, stratified on each study. The VPCs show that the model can reproduce the original data reasonably well. The pharmacokinetic model is considered valid for simulations of plasma exposure after AZ1 administration in healthy volunteers for the doses covered in the Phase I program.

The parameter estimates from the bootstrap of the final model were implemented in Berkeley Madonna and 1000 simulations were run for each dose of interest. The results of the simulations were transferred to R for calculation of the median (solid line) and 90% prediction intervals (PI) (dotted lines) of receptor occupancy at steady-state for the suggested doses in the Phase IIa study. The results of the simulated receptor occupancy versus time for 0.5 mg, 2 mg and 6 mg AZ1 are presented in Fig. 3. As is clear from the plot — the higher the dose is, the higher the maximal RO will be. It is also clear that the higher the dose, the smaller fluctuations will be achieved during a dosing interval.

Table III Key Steps in Model Building Process

Model	Reference model	Description	OFV	ΔOFV	Inter-individual variability (%)			Inter-occasion variability (%)	
					CL/F	V2/F	V3/F	CL/F	KA
1		Two compartment model with first order absorption and a lag-time — BASE MODEL	−8368.1		21.9	20.7	57.3	4.96	93.2
2	1	Add Japanese race on KA	−8435.7	−67.6					76.3
3	2	Add Black race on V3/F	−8570.5	−134.8			38.5		
4	3	Add weight on V2/F	−8644.0	−73.4		14.4			
5	4	Add weight on CL/F	−8714.5	−70.5	19.5			4.95	
6	5	Add Black race on Q/F	−8752.1	−37.6					
7	6	Add Japanese race on Q/F	−8777.7	−25.6					
8	7	Add Japanese race on V3/F	−8796.3	−18.7			33.2		

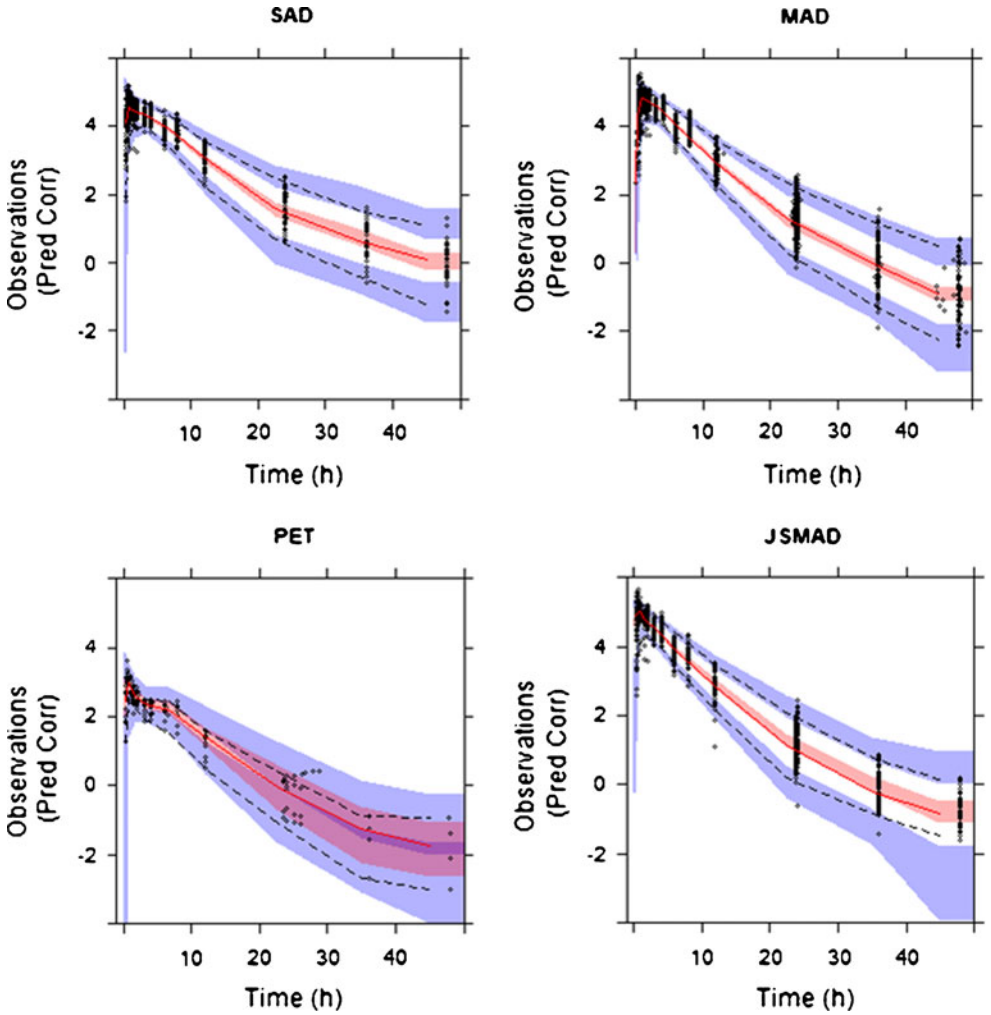

Fig. 2 Prediction corrected visual predictive checks for the pooled population PK analysis, stratified on each study. The *solid red line* represents the median prediction-corrected plasma concentration, and the *semitransparent red field* represents a simulation-based 95% confidence interval for the median. The observed 5% and 95% percentiles are presented with *dashed black lines*, and the 95% confidence intervals for the corresponding model predicted percentiles are shown as *semitransparent blue fields*. The observations are represented by *black circles*.

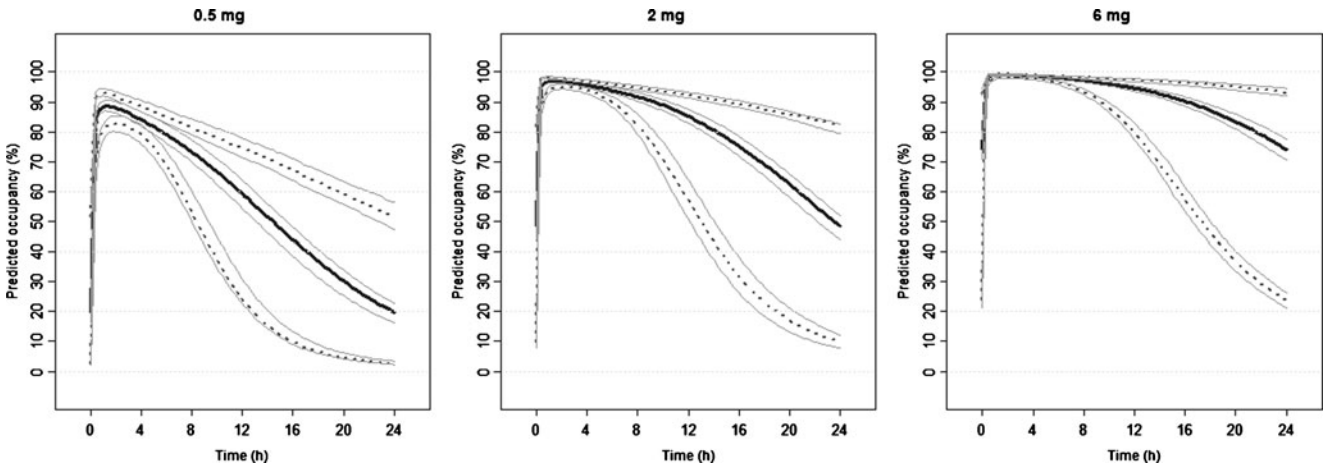

Fig. 3 Simulated RO *vs*. time profiles with 90% prediction intervals for 0.5 mg, 2 mg and 6 mg AZ1. The *black solid lines* represent the mean, and the *black dotted lines* the 90% prediction intervals of each dose, with a Ki-value of 1.14 nM. The *thin grey lines* represent the 95% confidence interval of the Ki-value.

Simulations of how the t1/2 altered a RO *vs*. time profile were carried out. The final PK model was used, and the values of clearance and volume of distribution were either kept or altered to yield a t1/2 that was the same as for AZ1, or approximately half or double the AZ1 half-life. The simulations are presented in Fig. 4. As is observable from the plots, with increasing t1/2, the possibility to have large diurnal fluctuations is decreased. With shorter t1/2, it is possible to both have high occupancy (above 90%) during the day, and low (below 60%) during night. It should be noted that the magnitude of diurnal fluctuations decrease with increasing the dose within panels of the same t1/2.

Sleep Assessment

The RO at night-time (16 h after morning dose) *vs*. the self-rated sleep assessment from the next morning for all days and all individuals is presented in Fig. 5. A relationship between predicted RO at night time and impaired sleep reported the morning after was indicated — with increasing RO, the proportion of subjects reporting 1 or 2 increases. In the lowest quantile approximately 7% of the subjects report poor sleep, while in the highest quantile this response is given by approximately 33% of the subjects.

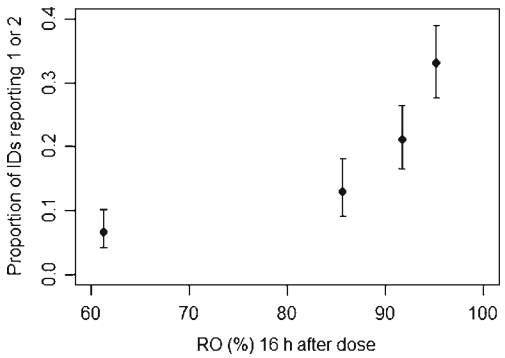

Fig. 5 The predicted RO at bedtime was divided into four bins and the proportion of individuals reporting 1 or 2 (i.e. poor sleep) was plotted against the median RO of each bin. The data are presented as point estimates and 95% confidence intervals.

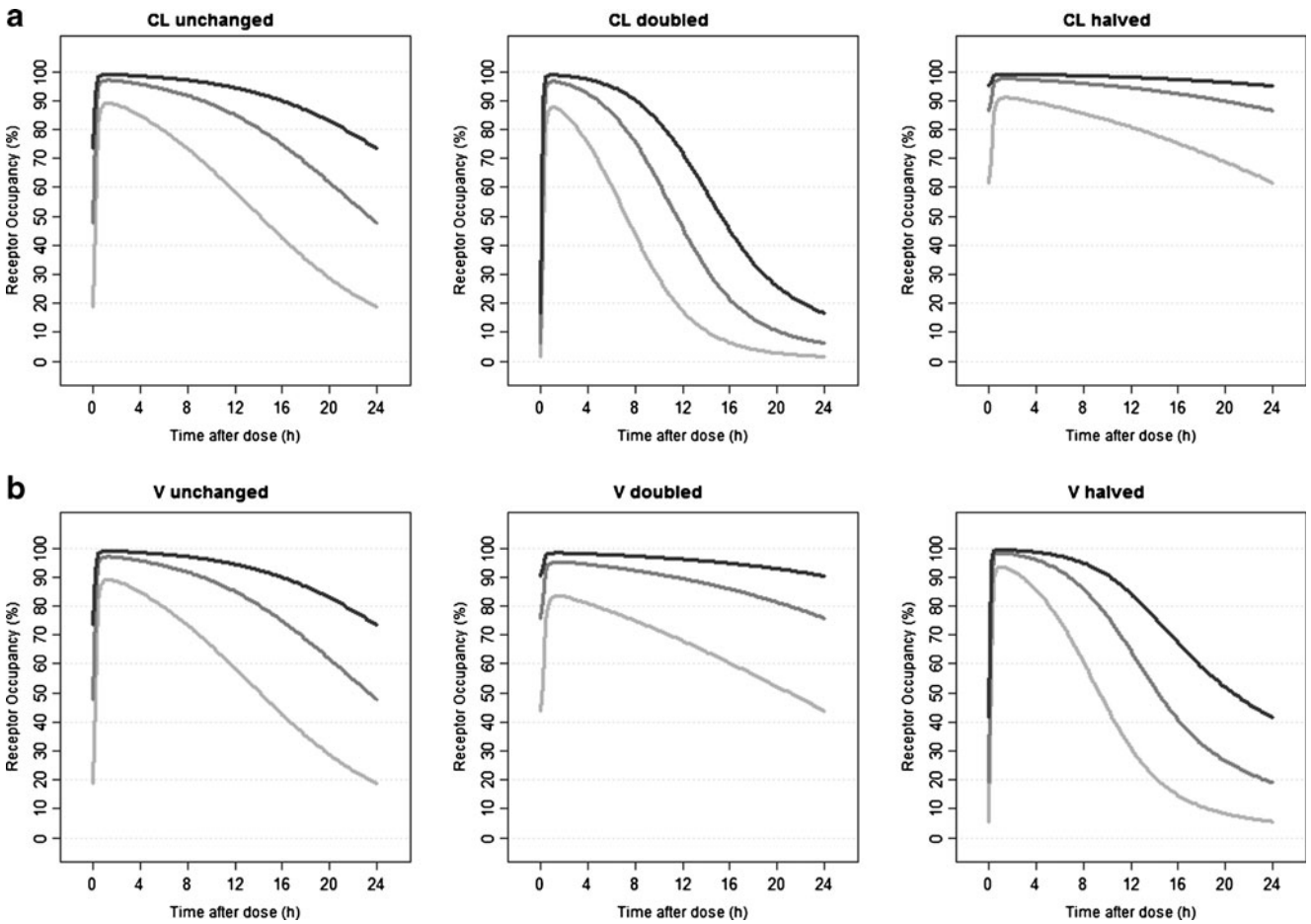

Fig. 4 Simulations of how difference in clearance and volume of distribution alter the RO *vs*. time profile. (**a**) shows how the RO *vs*. time profiles change when the clearance is doubled or halved. (**b**) shows how the RO *vs*. time profiles change when the volume of distribution is doubled or halved. The Ki is assumed to be the same in all simulations. The *black*, *dark grey* and *light grey lines* represent simulations of 6 mg, 2 mg and 0.5 mg AZ1, respectively.

DISCUSSION

For H3 *in vivo* antagonists, it is of key importance for success to select the optimal dose. While a high exposure is desired during the day for pro-cognitive effects, a maintained high night time exposure, and thereby RO, would have a high risk of leading to sleep disturbance and/ or insomnia. Sleep deprivation as such is well known to negatively impact cognition (14). Thus, treatment with an H3 antagonist for improving cognition needs to be well-balanced with respect to sleep impairment.

In this work, we show that by integration of population PK and the Ki-value from a human PET study, predictions can be made of RO *vs*. time for unstudied doses of a drug. This makes it possible to suggest doses with a wide range of predicted night-time RO to be used in a Phase II study, where the desired RO *vs*. time profile can be investigated. The importance of the relationship of dose, t1/2 and Ki-value is also emphasized in order to obtain favorable diurnal fluctuations in the RO *vs*. time relationship.

A pooled population PK model was developed based on data from healthy volunteer studies. The final model had stable parameter estimates in a bootstrap resampling procedure, and simulation based diagnostics with a VPC showed that the model could reproduce the data reasonably well. Important covariate relationships were identified, including weight on CL/F and V2/F, and the effect of race on Q/F and V3/F. One could argue that the race covariate in this case is confounded by weight. However, the impact of weight was also investigated on Q/F and V3/F, but as inclusion on race resulted in a greater drop in OFV and greater improvement in diagnostic plots, the covariate race rather than weight was kept in the model. No inter-individual variability in the Ki-value was reported in the PET study, and could thus not be included in the simulations of RO *vs*. time. Although not evaluated, the data in the RO *vs*. concentration plot in the PET study suggest that the inter-individual variability in Ki was limited (13).

A number of compounds affecting the H3 mechanism, including BF2.649, PF-03654746, GSK189254, GSK239512, MK- 0249, JNJ-17216498, and ABT-288, have advanced to the clinical area for the potential treatment of human cognitive disorders. H3 antagonists exhibited wake-promoting effects in humans and efficacy in narcoleptic patients, indicating target engagement, but some of them were not efficacious in patients suffering from attention-deficit hyperactivity disorder or schizophrenia. Pitolisant (BF2.649) delivered positive outcome in three phase IIa trials where it decreased daytime sleep associated with narcolepsy, Parkinson disease and sleep apnea (10). Preclinical studies have also shown that H3 antagonists activate intracellular signaling pathways that may have the ability to clinically improve cognitive function and perhaps even exert disease-modifying effects in Alzheimer's disease (for reviews, see (1,9)). The involvement of H3 receptors sleep-wake regulation was recently reviewed by Lin *et al.* (5).

During development of H3 antagonists frequent reports have stated that the half-life of the test drug has been major determinant of tolerability due the unwanted wakefulness effect during nighttime, for review, see (15). AZ1 is suggested to have a favorable tolerability index to fully test the H3 target potential, however, the relative efficacy contribution of the broader pharmacology including, effects on acetylcholine, dopamine and norepinephrine needs to be tested.

H3 occupancy may be useful for comparison of different H3 ligands. Thus, the short t1/2 of 5 h for AZ1 may be advantageous *vs*. other H3 compounds in clinical development that have reported half-lives >12 h. Hypothetically, if the risk of sleep disruption is indeed related to high H3 occupancy, as demonstrated in preclinical data, a shorter t1/2 should be advantageous since it allows greater circadian fluctuation thus allowing high daytime and low bedtime occupancy (16).

In this analysis, the influence of t1/2 on the RO *vs*. time profile was investigated by simulations of altered clearance or volume of distribution. The RO is related to the plasma concentration by a hyperbolic function where the concentration that yields 50% RO is described by the Ki-value. In general, the higher the dose, the higher RO, due to higher plasma concentration relative to Ki-value. Assuming the same t1/2, with higher doses, the concentration stays above the Ki-value for a longer time, and therefore the curve has a flatter appearance than doses that only yield concentrations in the range of the Ki-value or below. The t1/2 will determine the rate of decline both of plasma concentration, but also the occupancy of H3 receptors, as the t1/2 determines how long the drug concentration stays well above the Ki-value. If C_{trough} for a drug at steady-state is the same as the Ki-value, the RO_{trough} will be 50%. This reasoning is based on the characteristics of AZ1, but can be generalized for other substances as well. It is the relationship between the plasma concentration and the Ki-value that determines the shape of the RO profile, so if the Ki-value had been 5 times higher (and the PK model the same), the dose had to be 5 times higher to result in the same RO *vs*. time profiles.

From the simulations based on AZ1, it was evident that the shorter t1/2 of AZ1 compared to the competitors was only resulting in large diurnal fluctuations if the dose was not too high. Doses above 6 mg had a very flat RO *vs*. time profile, despite the t1/2 of 5 h, which is due to that the concentrations stays high above the Ki-value during the dosing interval. Using a very low dose would, in turn, not yield the desired high RO_{max}. The benefit of the simulations was enabling prediction of a dose range where the difference in night time RO was wide, while maintaining the high RO (90%) during the day.

Little information is available as to what an optimal RO *vs*. time profile would be, but it is anticipated that the RO should be below 70% to minimize sleep disturbances at night (17), in combination with an as-high-as-possible RO during day. As evident from the present self-reported sleep data, there seem

to be a relationship between night-time RO and the self-reported sleep quality. Reporting the proportion of responders of a binary variable has been demonstrated to be an informative way of presenting this type of data and could be used to explore the underlying exposure response relationship (18). One limitation with using self-reported sleep quality assessments is that it does not contain any actual numbers of hours of sleep time. Subject estimation of own actual sleep is frequently not consistent with objective measures of sleeping time. However, perceived night sleep gives a rough estimate of the effect of reduced sleep time, and may be used as a valid surrogate measure. It may also be argued that self assessment of sleep may not be a reliable measure of sleep time. However, high reliability in self assessment of sleep *vs*. direct measurements of sleep time has been demonstrated in healthy volunteers of variable ages (19). Even when using objective measures of sleep time, there is considerable inter-individual variability in this variable, as part of normal between-individual variation in sleep pattern. Also repeated measurements, as used in the present setting, are more reliable than a single night assessment. When repeatedly applying the presently used self assessment sleep time scoring system to measure pharmacodynamics effects, it was also taken into account that small differences of less than two scale steps were not considered clinically relevant changes. Any clinical interpretation of group data sleep scores should be done with caution.

It could also be argued that the H3 RO may not be directly related to all tentative pro-cognitive effects by H3 antagonists, as the direct H1 and H2 effects on CNS histamine release increasing attention and vigilance are the ones commonly measured in the short studies conducted so far. In addition, part of the downstream pharmacology includes the release of NA, Ach, serotonin and GABA, all important procognitive transmitters. The time course from transmitter release until a precognitive effect may be evident is not clear for these transmitters. It has not possible to separate histamine related and other procognitive effects in these early clinical pharmacology trials. When AZ1 was given as a single dose, higher doses (~50 mg) were needed to affect sleep compared to when AZ1 was given repeatedly (10–14 mg), where sleep was affected a few days after the first dose (Lindholm *et al.*, in preparation). As the RO is directly related to the plasma concentration and there is limited accumulation of AZ1 between day 1 and day 3, this suggests that there is not a direct link between target engagement (RO) and influence of sleep.

It should be reiterated that the relationships between H3 occupancy and neurochemical and clinical effects have not yet been characterized. Further clinical studies will be required to describe the PKPD relationships to optimize the benefit-risk profile of AZ1. However, the possibility to obtain high exposure and RO during daytime gives the opportunity to adequately test the hypothesis of cognitive enhancement in AD mediated by H3 inverse agonism.

CONCLUSION

In conclusion, by using population modeling and simulations of PK data and the Ki-value from a human PET study, predictions of the RO *vs*. time profile for unstudied doses of AZ1 was made. Using this methodology it was possible to suggest doses with expected large diurnal fluctuations in RO, i.e. high occupancy during day -for putative cognitive improvement- and low occupancy at night — to minimize the inherent H3 effects on sleep.

ACKNOWLEDGMENTS AND DISCLOSURES

All authors were at the time of preparation of this manuscript employees of AstraZeneca R&D. The analyses and studies described in this report were funded by AstraZeneca R&D.

REFERENCES

1. Brioni JD, Esbenshade TA, Garrison TR, Bitner SR, Cowart MD. Discovery of histamine H3 antagonists for the treatment of cognitive disorders and Alzheimer's disease. J Pharmacol Exp Ther. 2011;336(1):38–46.
2. Zhang M, Venable JD, Thurmond RL. The histamine H4 receptor in autoimmune disease. Expert Opin Investig Drugs. 2006;15(11):1443–52.
3. Passani MB, Lin JS, Hancock A, Crochet S, Blandina P. The histamine H3 receptor as a novel therapeutic target for cognitive and sleep disorders. Trends Pharmacol Sci. 2004;25(12):618–25.
4. Schlicker E, Werthwein S, Zentner J. Histamine H3 receptor-mediated inhibition of noradrenaline release in the human brain. Fundam Clin Pharmacol. 1999;13(1):120–2.
5. Lin JS, Sergeeva OA, Haas HL. Histamine H3 receptors and sleep-wake regulation. J Pharmacol Exp Ther. 2011;336(1):17–23.
6. Bonaventure P, Letavic M, Dugovic C, Wilson S, Aluisio L, Pudiak C, *et al*. Histamine H3 receptor antagonists: from target identification to drug leads. Biochem Pharmacol. 2007;73(8):1084–96.
7. Ligneau X, Landais L, Perrin D, Piriou J, Uguen M, Denis E, *et al*. Brain histamine and schizophrenia: potential therapeutic applications of H3-receptor inverse agonists studied with BF2.649. Biochem Pharmacol. 2007;73(8):1215–24.
8. Medhurst AD, Atkins AR, Beresford IJ, Brackenborough K, Briggs MA, Calver AR, *et al*. GSK189254, a novel H3 receptor antagonist that binds to histamine H3 receptors in Alzheimer's disease brain and improves cognitive performance in preclinical models. J Pharmacol Exp Ther. 2007;321(3):1032–45.
9. Esbenshade TA, Browman KE, Bitner RS, Strakhova M, Cowart MD, Brioni JD. The histamine H3 receptor: an attractive target for the treatment of cognitive disorders. Br J Pharmacol. 2008;154(6):1166–81.
10. Schwartz JC. The histamine H3 receptor: from discovery to clinical trials with pitolisant. Br J Pharmacol. 2011;163(4):713–21.

11. Zoethout RW, Iannone R, Bloem BR, Palcza J, Murphy G, Chodakewitz J, *et al*. The effects of a novel histamine-3 receptor inverse agonist on essential tremor in comparison to stable levels of alcohol. J Psychopharmacol. 2012;26(2):292–302.
12. Bergstrand M, Hooker AC, Wallin JE, Karlsson MO. Prediction-corrected visual predictive checks for diagnosing nonlinear mixed-effects models. AAPS J. 2011;13(2):143–51.
13. Jucaite A, Takano A, Bostrom E, Jostell KG, Stenkrona P, Halldin C, *et al*. AZD5213: a novel histamine H3 receptor antagonist permitting high daytime and low nocturnal H3 receptor occupancy, a PET study in human subjects. Int J Neuropsychopharmacol. 2012;10:1–9.
14. Fortier-Brochu E, Beaulieu-Bonneau S, Ivers H, Morin CM. Insomnia and daytime cognitive performance: a meta-analysis. Sleep Med Rev. 2012;16(1):83–94.
15. Kuhne S, Wijtmans M, Lim HD, Leurs R, de Esch IJ. Several down, a few to go: histamine H(3) receptor ligands making the final push towards the market? Expert Opin Investig Drugs. 2011;20(12):1629–48.
16. Le S, Gruner JA, Mathiasen JR, Marino MJ, Schaffhauser H. Correlation between ex vivo receptor occupancy and wake-promoting activity of selective H3 receptor antagonists. J Pharmacol Exp Ther. 2008;325(3):902–9.
17. Iannone R, Renger J, Potter W, Dijk D, Boyle J, Palcza J, et al. The relationship between brain receptor occupancy (RO) and alerting effects in humans support MK-0249 and MK-3134 as inverse agonists at the histamine subtype-3 pre-synaptic receptor (H3R). ACNP48th Annual Meeting; Dec 6–10; Hollywood, FL: American College of Neuropsychopharmacology, Nashville, TN.; 2009.
18. Mehrotra S, Florian Jr J, Gobburu J. Don't get boxed in: commentary on the visual inspection practices to assess exposure-response relationships from binary clinical variables. J Clin Pharmacol. 2012;52(12):1912–7.
19. Manconi M, Ferri R, Sagrada C, Punjabi NM, Tettamanzi E, Zucconi M, *et al*. Measuring the error in sleep estimation in normal subjects and in patients with insomnia. J Sleep Res. 2010;19(3):478–86.